Available online at www.sciencedirect.com
SCIENCE DIRECT
Journal of Constructional Steel Research 62 (2006) 1026–1038
JOURNAL OF CONSTRUCTIONAL STEEL RESEARCH
www.elsevier.com/locate/jcsr

Panel shear strength of steel coupling beam–wall connections in a hybrid wall system

Park Wan-Shin[a], Yun Hyun-Do[b,*]

[a] *Department of Civil and Environmental Engineering, University of Cincinnati, 765 Baldwin Hall, Cincinnati, OH 45221, USA*
[b] *Department of Architectural Engineering, Chungnam National University, Daejeon, 305-764, Republic of Korea*

Received 21 March 2005; accepted 3 January 2006

Abstract

One of the most common types of hybrid systems is represented by a hybrid coupled shear wall consisting of steel coupling beams and reinforced concrete shear walls, known as a hybrid wall system. This paper addressed the shear strength of connection between structural steel coupling beams and reinforced concrete shear walls. No specific guidelines are available for predicting the panel shear strength of steel coupling beam–wall connections in a hybrid coupled shear wall system. The panel shear strength of steel coupling beam–wall connections in a hybrid coupled shear wall system is examined through results of an experimental research programme where three 2/3-scale specimens were tested under cyclic loading. Panel shear strength reflects enhancement achieved through mobilization of the reinforced concrete panel using face bearing plates and/or horizontal ties in the panel region of steel coupling beam–wall connections. The results and discussion presented in this paper are compared with ASCE design guidelines for RCS composite joints, which form a similar structural system. Finally, this paper provides the background for design guidelines that include a design model to calculate the panel shear strength of steel coupling beam–wall connections.

Keywords: Steel coupling beam–wall connections; Panel shear strength; Hybrid coupled shear walls; Steel web panel; Concrete compression struts; Concrete compression field

1. Introduction

This paper is the second of two papers addressing the behavior and design of steel coupling beam–wall connections for hybrid coupled shear walls in a panel shear panel. The first paper [1] provides a description of the hybrid coupled shear walls. Recent experimental research [2–4] on steel coupling beam–wall connections which served seismic performance is also summarized in the companion paper. As reported here, experimental tests have demonstrated that connection detail with face bearing plates and horizontal ties can result in significant enhancement to the strength of steel coupling beam–wall connections.

From testing programmes conducted in the late 1980s [5,6], the ASCE Task Committee on Design Criteria for Composite Structures in Steel and Concrete published a set of design guidelines for joints in RCS composite frames [7]. However, no specific guidelines are available for computing the panel shear strength of steel coupling beam–wall connections because of a lack of test data for hybrid coupled shear walls.

The objective of this research was to investigate the panel shear strength of steel coupling beam–wall connections governed by panel shear failure. Based on the resistance mechanism of similar structural systems (RCS structures), the shear resistance mechanism of steel coupling beam–wall connections is investigated. To evaluate the contribution of each mechanism, depending upon connection details, an experimental study was carried out. The results and discussion presented in this paper are compared with ASCE design guidelines for RCS composite joints, which form a similar structural system. Finally, this paper provides background for design guidelines that include a design model to calculate the panel shear strength of steel coupling beam–wall connections.

* Corresponding author. Tel.: +82 42 821 5622; fax: +82 42 823 9467.
E-mail address: wiseroad@cnu.ac.kr (H.-D. Yun).

0143-974X/$ - see front matter © 2006 Elsevier Ltd. All rights reserved.
doi:10.1016/j.jcsr.2006.01.006

2. RCS composite connections

2.1. Previous research studies

During the 1990s and early 2000s, a large number of research programmes on RCS composite joints have been conducted in Japan and US, primarily by private construction companies, and therefore the results are seldom available in English in the technical literature. During the mid-1990s, as a consequence of the advantages recognized in RCS structures, an extensive research programme, focused primarily on interior RCS composite joints, was undertaken in the United States and Japan. In Japan, several researchers [8–10] have also investigated the seismic behaviour of RCS composite joints and frames. The behaviour of exterior RCS composite joints has been analytically studied by Noguchi et al. [11–13] on the basis of experimental results from tests performed at Chiba University and the Building Research Institute in Japan. The first important attempts to study the behaviour of RCS composite joints in the United States were reported at the University of Texas at Austin by Sheikh et al. [14]. Seventeen interior RCS composite joints with various joint details were tested under monotonic and cyclic loading. The joint details included face bearing plates, steel columns embedded in the RC column, dowel bars, and shear studs attached to the beam flange. Kanno and Deierlein [15] reported the testing of 19 interior RCS composite joints, subjected to cyclic loading, at Cornell University. This research investigated different joints and has extended the joint behaviour models to account for different joint details and different stiffeners and shear stud arrangements, as well as for the presence of transverse floor beams. The results from these experimental programmes led to the ASCE design recommendations [7] for RC column–beam moment connections in composite frames. Montesions et al. [16] evaluated the effectiveness of the design procedure through the design and reversed-cyclic load testing of two RCS column–beam–slab subassemblies. The ability of the design equations to limit joint deformations, and thus damage, was evaluated, as well as the contributions from different mechanisms to total storey drift. In addition, Moore and Goasain [17] have shown that the RCS composite joint details with band plates possess excellent strength and stiffness retention capacity under large load reversals.

2.2. ASCE design guidelines for RCS joints

The ASCE Task Committee on Design Criteria for Composite Structures in Steel and Concrete [7] published a series of design guidelines for joints in RCS composite frames. These guidelines were intended for determining the strength of interior and exterior RCS composite joints and the detailing of face bearing plates and horizontal ties in those joints. The nominal shear panel strength of the steel web, V_{sn}, inner concrete compression strut, V_{csn}, and outer concrete compression field, V_{cfn}, specified in the ASCE design guidelines are as follows.

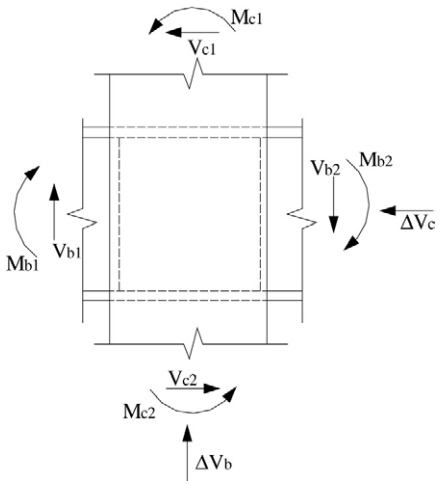

Fig. 1. RCS composites joints design forces (Sheikh, 1989).

(1) Steel web panel (V_{sn})

The nominal strength of the steel web panel, V_{sn}, is calculated as follows:

$$V_{sn} = 0.6 F_{ysp} t_{sp} jh \tag{1}$$

where F_{ysp} and t_{sp} are the yield strength and thickness of the steel panel, respectively, and the effective joint depth, jh, is determined through an iteration procedure based on external load and joint properties.

(2) Concrete compressive strut (V_{csn})

The nominal strength of the concrete compression strut mechanism, V_{csn}, is calculated as follows:

$$V_{csn} = 1.7\sqrt{f_c'} b_p h \le 0.5 f_c' b_p d_w \tag{2}$$

where f_c' and $\sqrt{f_c'}$ are the joint concrete compressive strength, b_p is the effective width of the face bearing plates, h is the column depth, and d_w is the height of the steel beam web.

(3) Concrete compression field (V_{cfn})

The nominal strength of the concrete compression field mechanism, V_{cfn}, is calculated as follows:

$$V_{cfn} = V_c' + V_s' \le 1.7\sqrt{f_c'} b_o h, \tag{3}$$

$$V_c' = 0.4\sqrt{f_c'} b_o h, \tag{4}$$

$$V_s' = A_{sh} F_{ysh} 0.9h/s_h \tag{5}$$

where b_o is the width of the outer concrete panel, A_{sh} is the cross-section area of joint ties measured in a plane perpendicular to the beam axis, F_{ysh} is the yield strength of joint ties, and s_h is the spacing of joint ties.

The horizontal shear strength is considered adequate if the following equation is satisfied:

$$\sum M_c - V_b jh \le \phi[V_{sn} d_f + 0.75 V_{csn} d_w + V_{cfn}(d + d_o)] \tag{6}$$

$$\sum M_c = (M_{c1} + M_{c2}), \tag{7}$$

$$V_b = (V_{b1} + V_{b2})/2 \tag{8}$$

where M_{c1}, M_{c2}, V_{b1}, and V_{b2} are the column moments and beam shear forces, as shown in Fig. 1. The distance, d_f, is the centre-to-centre distance between the beam flanges, d is the total height of the steel beam, d_o is the additional effective joint

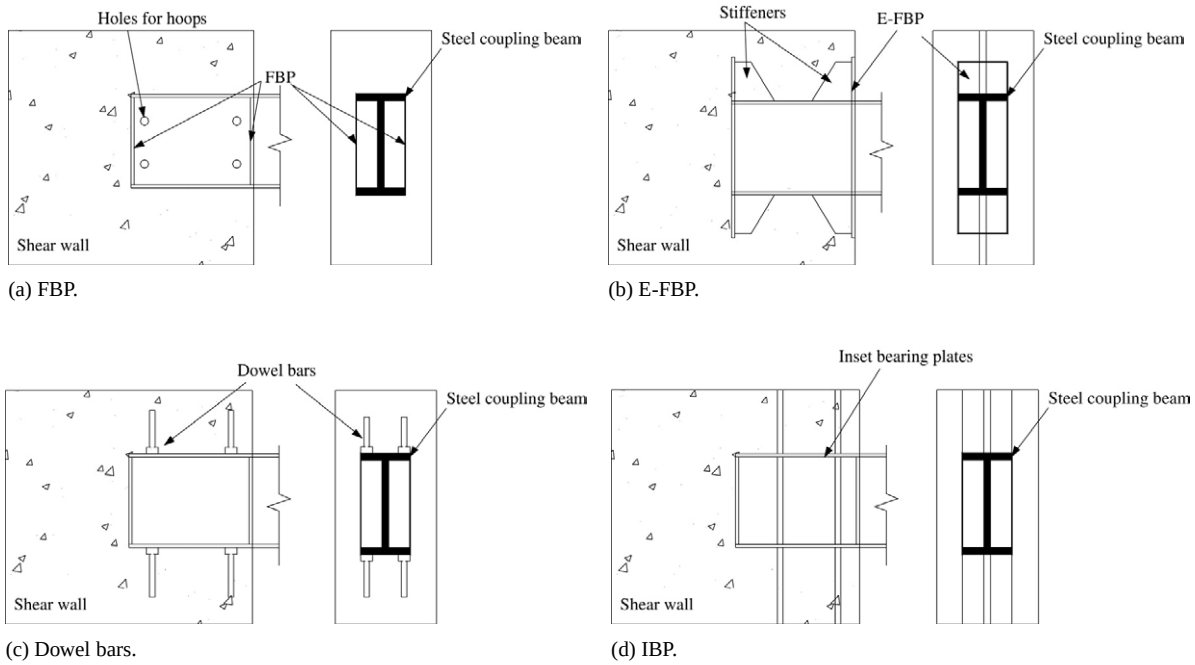

Fig. 2. Reinforcement details of connection.

depth provided by attachments to beam flanges, and jh is the horizontal distance between the bearing force resultant.

3. Resistance mechanism of steel coupling beam–wall connections

No specific guidelines are available for computing the panel shear strength of steel coupling beam–wall connections because of a lack of test data for hybrid coupled shear walls, but references to previous studies show the adequacy of models proposed by the ASCE design guidelines [7] for reinforced concrete columns and steel beams, and RCS composite joints, which form a similar structural system [16].

3.1. Connection details

Generally, the connection details used to mobilize joint shear in a hybrid coupled shear wall system are as shown in Fig. 2. Face bearing plates (FBPs), located at the face of the concrete shear walls, mobilize a concrete compression strut between the steel coupling beam flanges through direct bearing, as shown in Fig. 2(a). As shown in this section, the face bearing plates can vary in width and may be either full height or split for ease of fabrication. The extended face bearing plates (E-FBPs) shown in Fig. 2(b) mobilize the concrete compression field outside the flanges through struts. Other attachments, such as welded shear studs or inset bearing plates (IBPs), can enhance panel shear strength in a similar manner, as shown in Fig. 2(c) and (d). Vertical connection reinforcement attached to the steel coupling beam, as shown in Fig. 2(c), increases the bearing strength when bearing failure controls. Such reinforcement resists compression where the beam flange bears on the concrete, and it resists tension at the opposite flange where gaps typically open between the steel coupling beam and concrete shear walls. Vertical reinforcement of connection may consist of standard reinforcing bars, Dywidag reinforcing bars, structural stud bolts, or other elements attached to the steel coupling beam.

3.2. Failure modes

The behaviour of steel coupling beam–wall connections is characterized by two primary modes of failure, as shown in Fig. 3. As shown in Fig. 3(a), the panel shear failure of steel coupling beam–wall connections is similar to that typically associated with structural steel beams and reinforced concrete column joints for composite frames [6]. As shown in Fig. 3(b), the bearing failure occurs at locations of high compressive stress and permits rigid body rotation of the steel beam within the concrete shear walls. As will be described, vertical reinforcement of steel coupling beam–wall connections is one means of strengthening against bearing failure.

3.3. Panel shear mechanism

Fig. 4 shows idealized panel shear mechanisms for steel coupling beam–wall connections. Panel shear is carried through the connection by a combination of the three mechanisms shown in Fig. 4: the steel web panel, the concrete compression strut, and the concrete compression field. In general, the relative participation of each mechanism depends upon connection details.

The steel web panel acts similarly in hybrid and structural steel connections, as shown in Fig. 4(a). The web is idealized as carrying pure shear stress over an effective panel length, jh, which is dependent on the location and distribution of vertical bearing stresses.

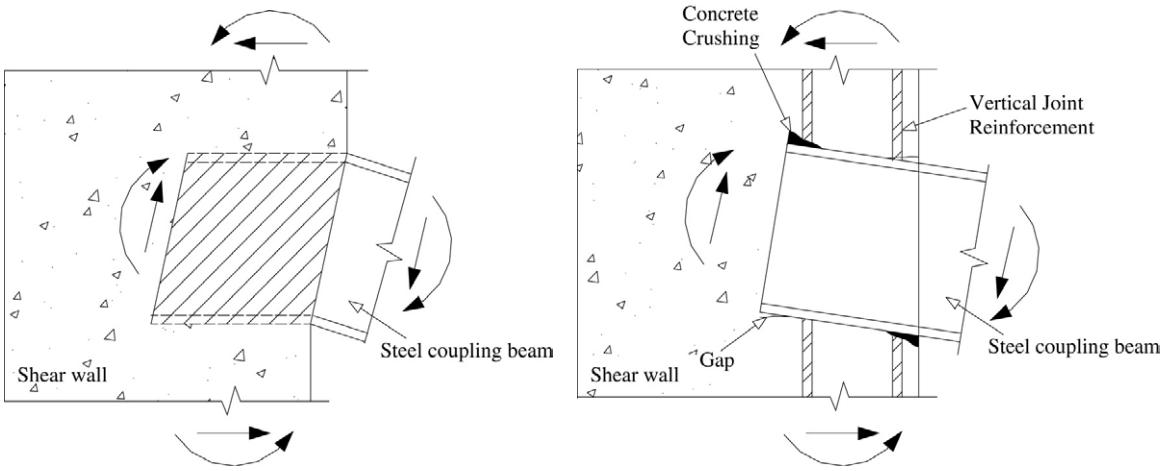

(a) Panel shear failure. (b) Vertical bearing failure.

Fig. 3. Failure mode of connection.

The concrete compression strut is similar to the mechanism used to model shear in composite frame connections, as shown in Fig. 4(b). In connections of hybrid coupled shear wall systems, the concrete strut is mobilized by face bearing plates, attached to the steel coupling beam, that bear against the concrete. As will be described, the location and width of the face bearing plates determine how effectively the concrete compression strut is mobilized in resisting shear force.

The concrete compression field consists of several compression struts that act with horizontal ties to form a truss mechanism, as shown in Fig. 4(c). The concrete compression field is mobilized in the region outside the steel coupling beam flanges. This mechanism is similar to truss models for shear in reinforced concrete beams where the strength is limited by the sum of concrete and reinforcing steel components. Shear is transferred horizontally from the beam flange to the compression field through bearing against the coupled shear walls.

4. Experimental program

4.1. Test specimens and setup

The overall concrete shear wall and steel coupling beam dimensions of specimens used in this study are identical to those presented in previous research [1]. The test variables and details used in this study are summarized in Table 1 and Fig. 5. The steel coupling beam was used in the tests to force failure in the connection regions, but in design, the members would be proportional so that failure occurs in the beams before the connection or wall strength is reached.

The specimens were cast vertically, but typical construction joints in the wall around the connections were not reproduced. Ready-mix concrete with a minimum specified 28-day compressive strength of 30.0 MPa was used for each of the three specimens. The measured concrete strength and the elastic modulus were tested using the method defined in the ASTM standards. The horizontal and vertical reinforcement consisted of 13 mm diameter deformed bars. Tension tests were conducted on full-sized bar samples in accordance with ASTM Standard A370 to determine the yield strength, ultimate strength, and total elongation. The observed material properties are reported in Fig. 6. A schematic diagram of the test apparatus and the observed displacement history of the tests are also identical to those presented in previous research [1].

4.2. Hysteretic response

Fig. 7 shows the failure modes and hysteretic response for specimens PSF, PSFF, and PSFFT. All specimens exhibited severe damage in the connection region at the end of the test. The severity of the damage observed in the connection region for all specimens is shown clearly. Specimen PSF sustained lower panel shear force, as the regions of the walls adjacent to the steel coupling beam flanges exhibited more damage than did specimens PSFF and PSFFT. From the observed failure modes, specimen PSFFT, with face bearing plates and horizontal ties in the panel region, was a more viable candidate than specimens PSF and PSFF for rehabilitation or retrofitting when considering the degree of building damage. The load–rotation angle response for specimen PSF, which is representative of the cyclic tests, indicated that the steel coupling beam–wall connections are not very ductile, as shown in Fig. 7(a). Specimen PSFF showed a 47% increase of panel shear strength in comparison with specimens PSF, as shown in Fig. 7(b). Specimen PSFFT, which had face bearing plates and horizontal ties within the width of the steel coupling beams, showed no degradation of strength throughout the tests and only a small degradation of stiffness during repeated cycles at the same rotation angle level, in comparison with specimens PSF and PSFF.

The relationship between normalized measured load and rotational angle is shown in Fig. 8. Fig. 8(a) shows average values of $V_{(\text{test})}/V_{n(\text{ASCE})}$ for specimens PSF, PSFF, and PSFFT of 1.14, 1.06, and 1.08, respectively. Compared with the test results of Montesinos et al. [16], specimen PSFFT and specimen 4, which had face bearing plates and horizontal ties in

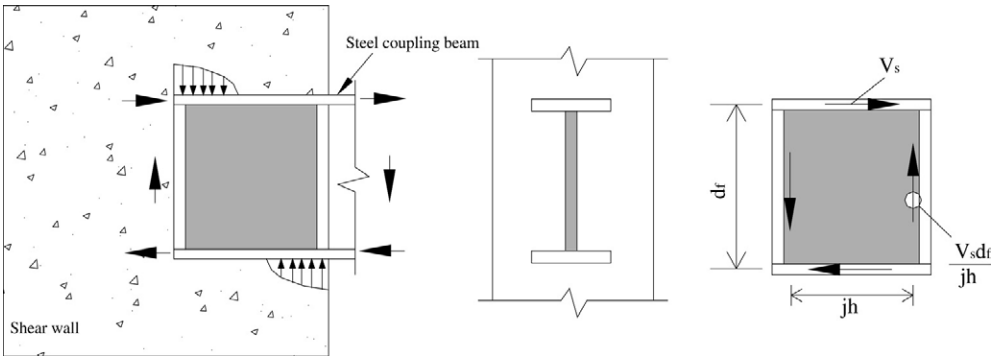

(a) Steel web panel.

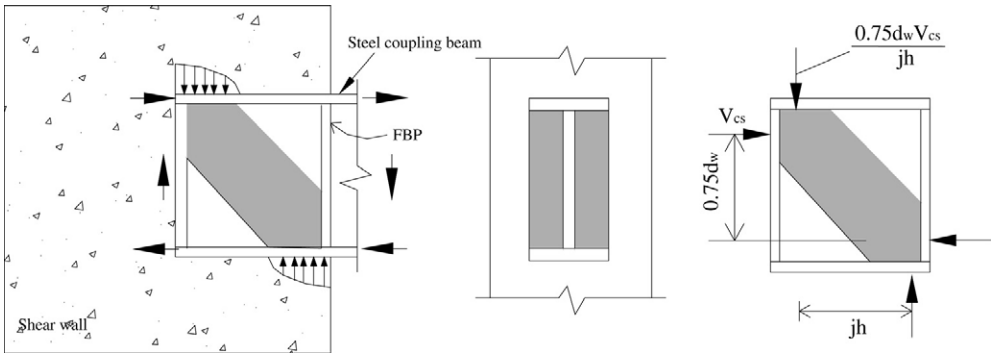

(b) Concrete compression strut.

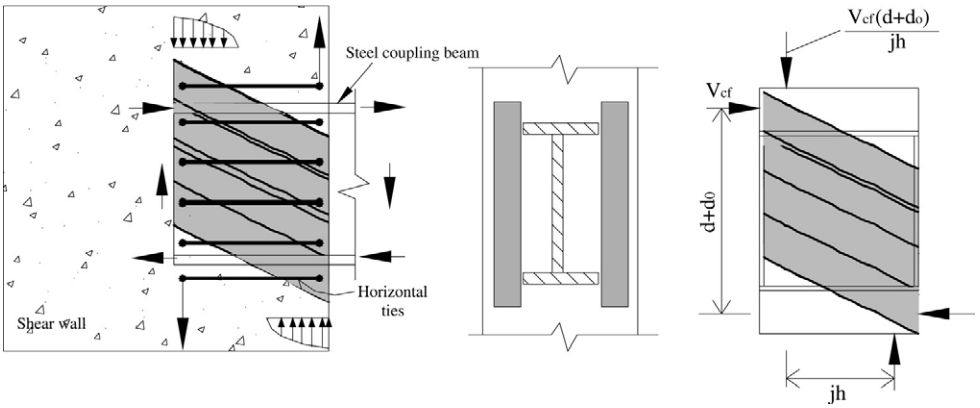

(c) Concrete compression field.

Fig. 4. Idealized panel shear mechanisms.

Table 1
Test variables

Specimen name	Detail of connection ①	②	③	f'_c (MPa)	Beam section (mm × mm × mm × mm)	Wall thickness (mm)	Loading method	Eccentricity of vertical load *e* (mm)	Predicted failure mode
PSF	•	–	–	30.0	H-175 × 175 × 5 × 15	300	Cyclic	+150	Panel shear failure
PSFF	•	•	–	30.0	H-175 × 175 × 5 × 15	300	Cyclic	+150	Panel shear failure
PSFFT	•	•	•	30.0	H-175 × 175 × 5 × 15	300	Cyclic	+150	Panel shear failure

①ST: Stud bolts; ②FBP: Face bearing plate; ③HT: Horizontal ties.

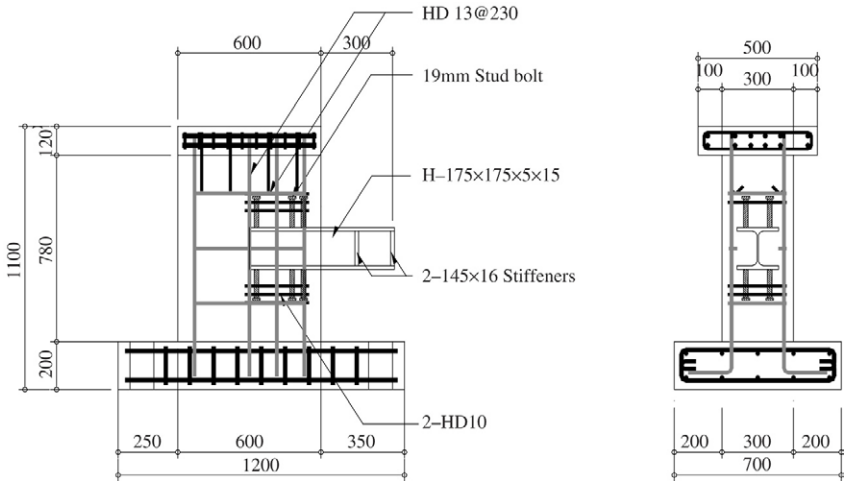

(a) Specimen PSF.

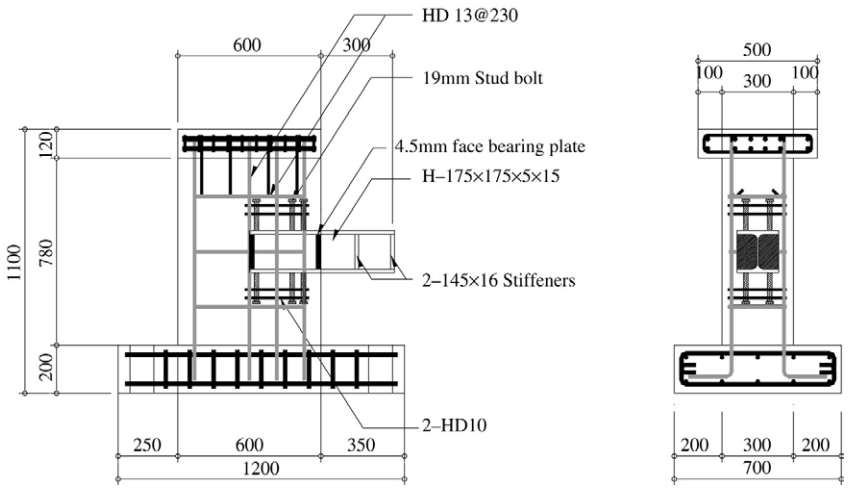

(b) Specimen PSFF.

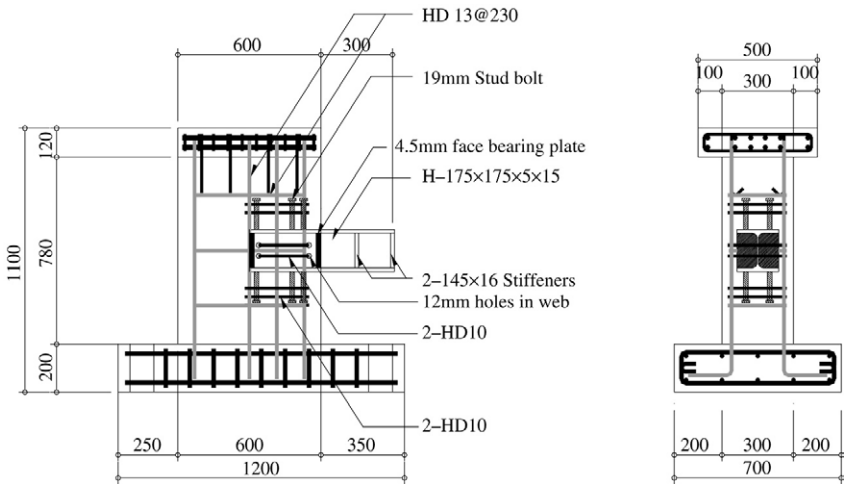

(c) Specimen PSFFT.

Fig. 5. Details of steel coupling beam–wall connections (unit; mm).

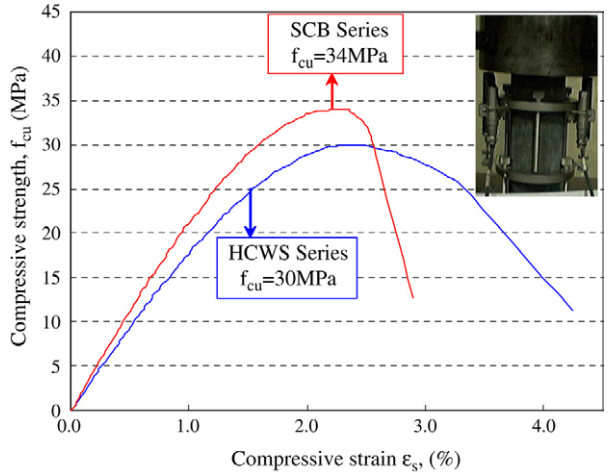

(a) Concrete.

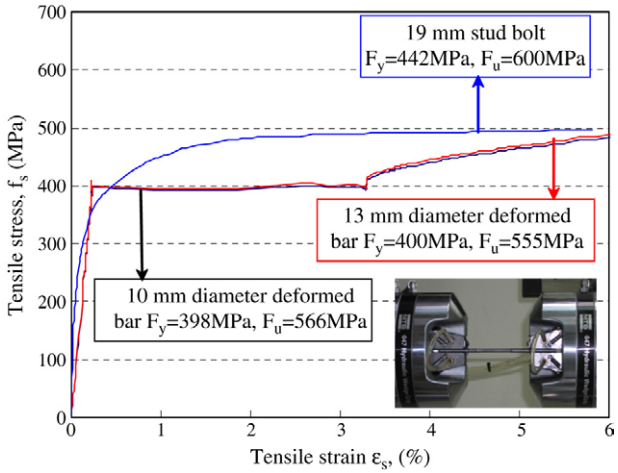

(b) Reinforcing steel.

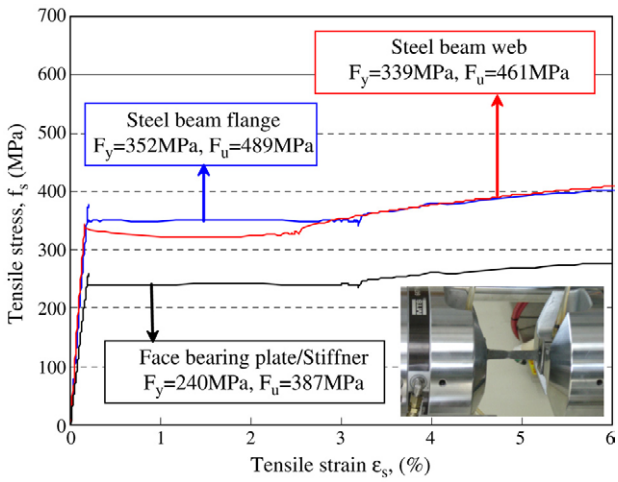

(c) Steel coupling beam flange, web, and FBP/Stiffener.

Fig. 6. Material properties of concrete and steel.

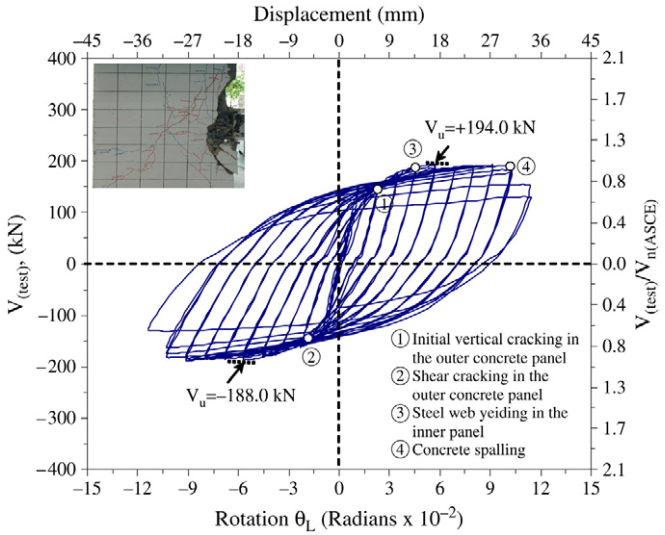

(a) Specimen PSF.

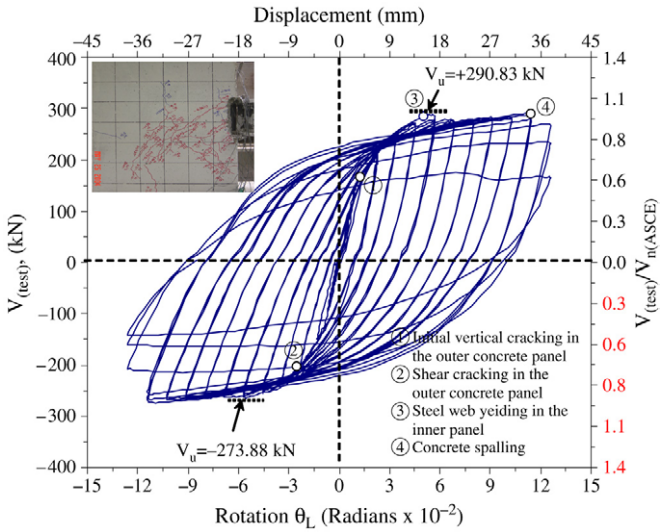

(b) Specimen PSFF.

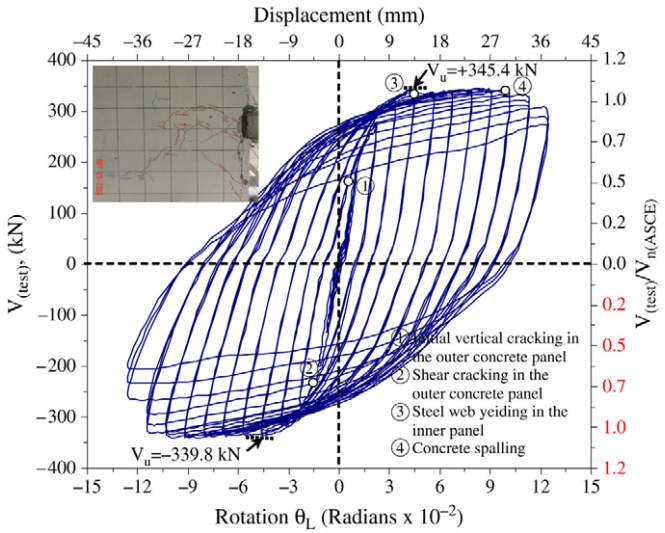

(c) Specimen PSFFT.

Fig. 7. Load–deformation hysteresis loops.

the connection regions, showed more stable responses, without significant strength degradation beyond ultimate load, than specimen PSF and specimen 1, as shown in Fig. 8(b).

4.3. Stresses of embedded steel beam web

Fig. 9 shows the distribution of stresses in the embedded steel beam web of specimens PSF, PSFF, and PSFFT. The strains in the embedded steel web of steel coupling beam–wall connections were measured at three different locations, 50 mm, 150 mm, and 250 mm inside the walls, by means of rosette strain gauges, in order to determine the distribution of stresses. It can be seen that the distribution of stresses does not follow a symmetrical pattern, with the higher stresses recorded in the front half of the embedded steel coupling beam length. In specimen PSF with normal detail connection, significant deterioration of the connection started to take place after yielding of the steel web panel occurred, characterized by a rapid increase in the width of diagonal cracks, and spalling of the concrete, as shown in Fig. 9(a). In specimen PSFF, yielding of the steel web panel started to occur at a rotation angle of about 0.045 rad, spreading rapidly toward the wall face as the load was increased, as shown in Fig. 9(b). The stresses near the back face of the connection (point A) were approximately 20% lower than those measured at the front face (point C). Compared with those in specimens PSF, PSFF, and PSFFT, the distribution of steel web stresses was sensitive to the changes in the connection detail, as shown in Fig. 9(c).

4.4. Strains of horizontal ties

Fig. 10 shows the distribution of strains in the horizontal ties at two different locations inside the connection for specimen PSFFT. The pre-cracking behaviour is characterized by negligible strains because of the small tensile stresses acting in the connection, which are primarily resisted by the concrete and the web of the steel beam. After the first crack occurred, the tensile stresses previously acting in the concrete were primarily resisted by the horizontal ties, leading to a sudden increase in the measured strains in the horizontal ties, as indicated by the nearly linear relationship between the applied beam shear and the average horizontal tie strain. In Fig. 10(a), the different responses can be observed for the positive and negative loading directions after several cracks formed in the connection. Fig. 10(b) shows the strains measured in the bottom U-shaped ties for specimen PSFFT. A similar pre-cracking and post-cracking response, compared with that for the top horizontal ties, can be observed. However, at the bottom horizontal ties, larger tensile strains were measured for the positive loading direction. The changes in tensile strains for both directions of loading primarily depended on the cracking pattern and the location of the cracks with respect to the strain gauges.

4.5. Stresses of stud bolts

Strain gauge readings for stud bolts adjacent to the connection are shown in Fig. 11. Also shown is the theoretical

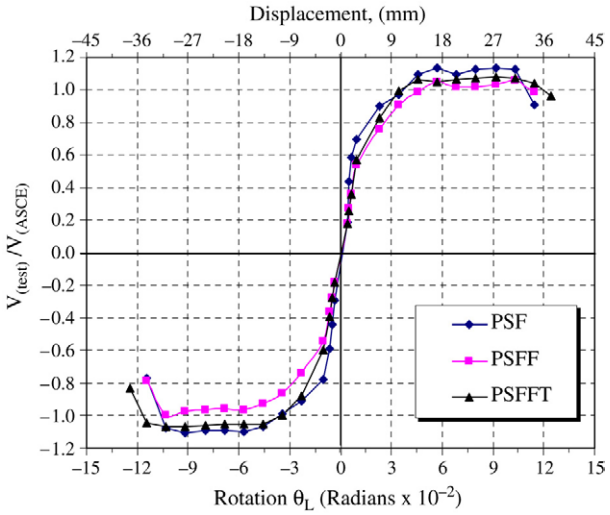

(a) Specimens PSF, PSFF, and PSFFT.

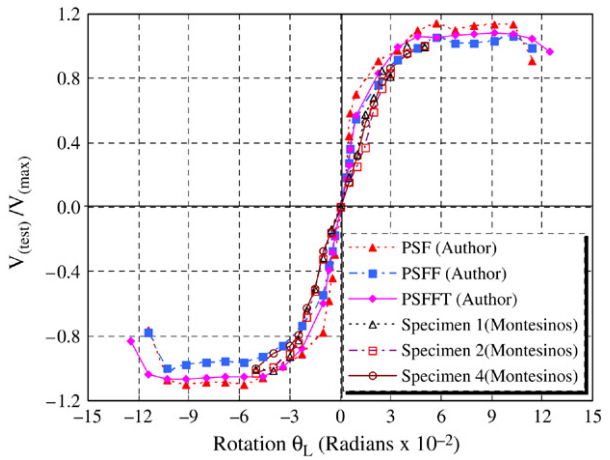

(b) Normalized envelope curve.

Fig. 8. Strength characteristics.

stress of stud bolts calculated using classical bending theory for all specimens. When the connection was loaded as shown in the figure, the upper gauge recorded tension and the lower gauge recorded compression. Initially, the measured tensile stress was slightly less than the theoretical stress, probably because of tension in the concrete and an unequal distribution of force between all the stud bolts, neither of which is accounted for by classical beam theory. The difference in the measured and theoretical bar stress indicates that transfer of force to the stud bolts in the steel coupling beam–wall connections was roughly one-half that predicted by theory. In the tests, loss in transfer appeared to result from concrete cracking, which tended to isolate the corner stud bolts from the connection region.

5. Panel shear strengths

Panel shear strengths of steel coupling beam–wall connections are governed by a combination of three mechanisms:

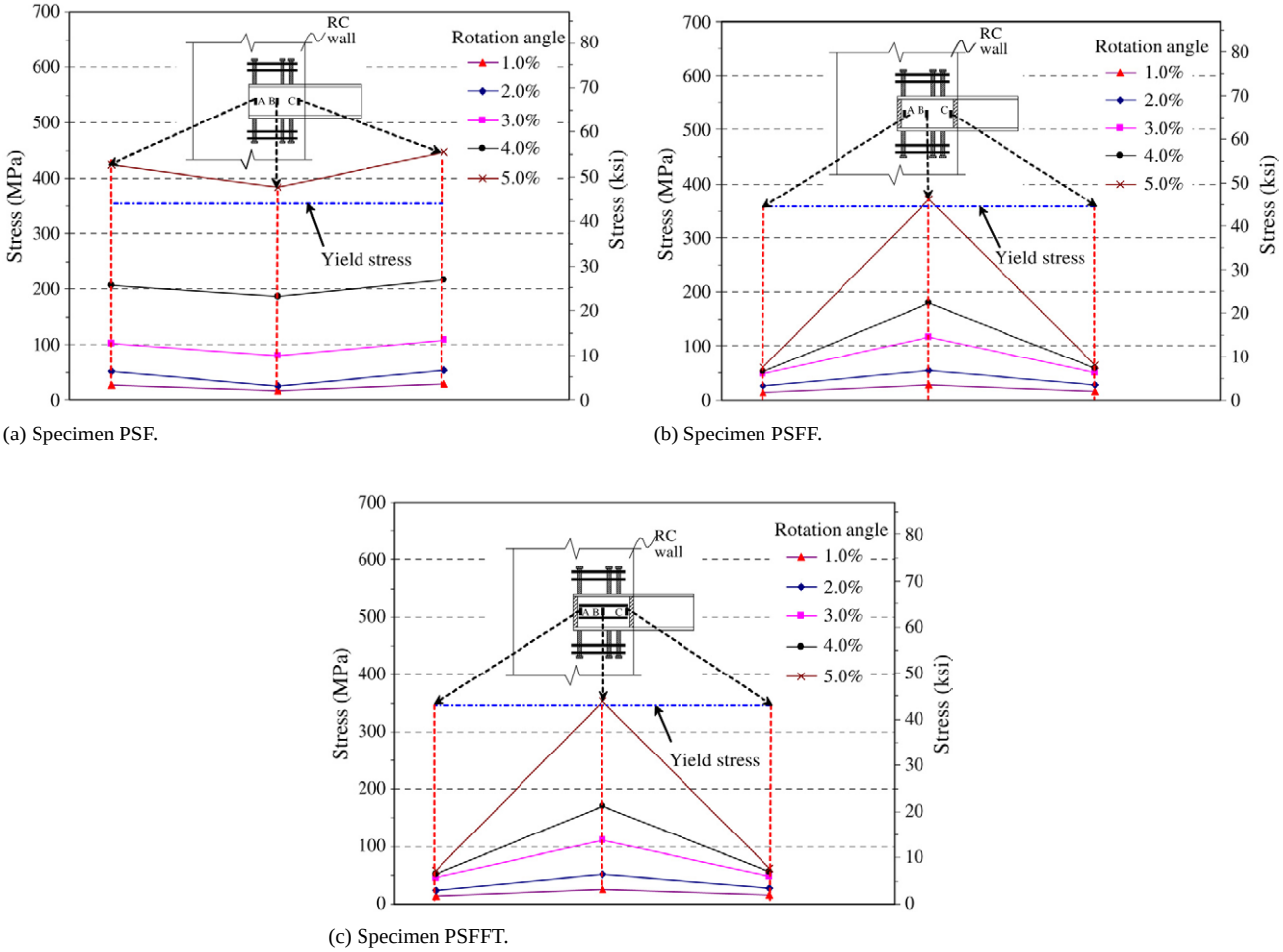

(a) Specimen PSF.

(b) Specimen PSFF.

(c) Specimen PSFFT.

Fig. 9. Stresses of steel web.

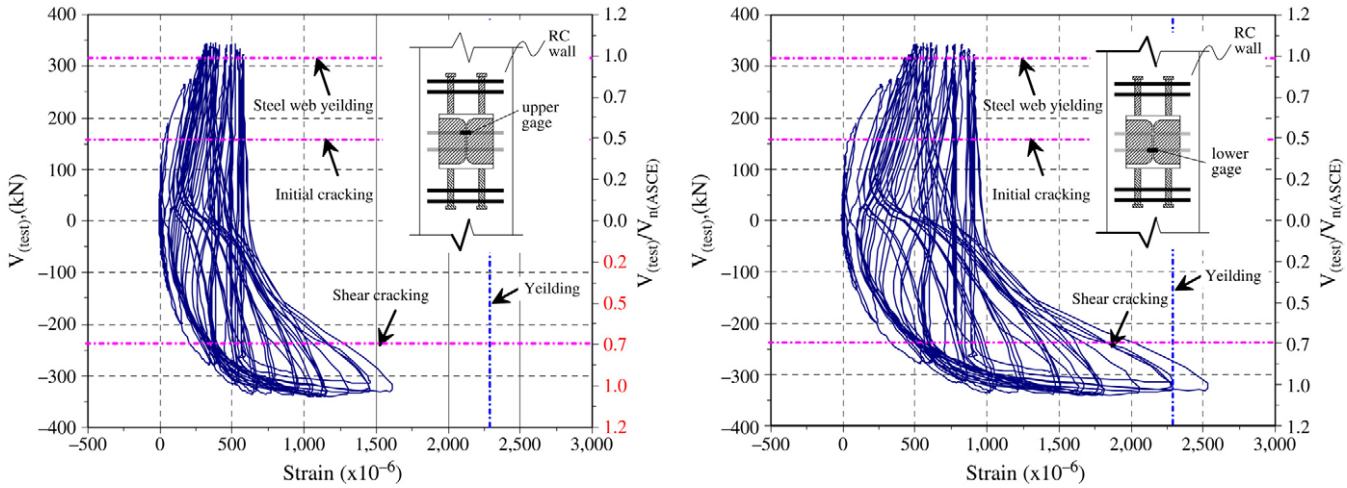

(a) Top horizontal tie.

(b) Bottom horizontal tie.

Fig. 10. Strains in horizontal ties inside connection (specimen PSFFT).

the steel web panel, the concrete compression strut, and the concrete compression field. A description of the connection details and test results of the panel shear strengths is presented in Table 2.

5.1. Concrete compression strut

Specimen PSF consisted of a plain steel beam and thus had no means other than friction and adhesion of transferring

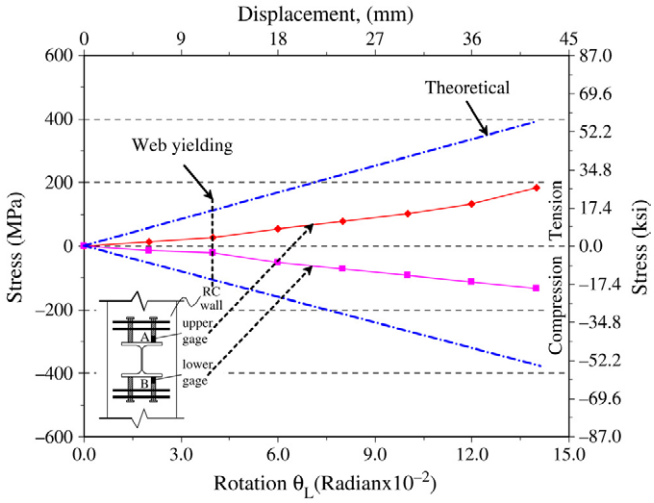

(a) Specimen PSF.

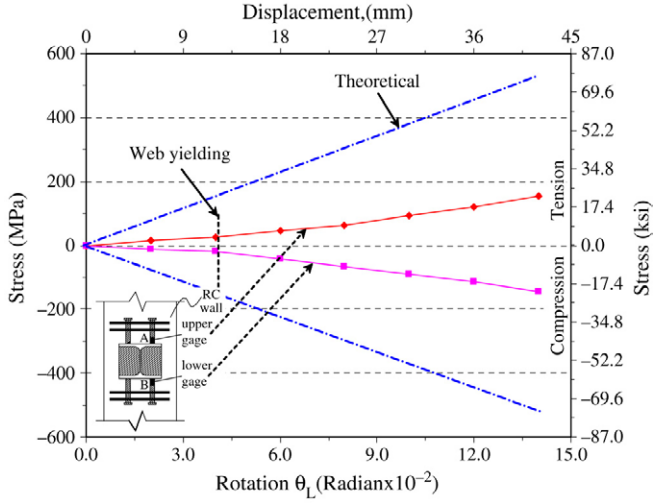

(b) Specimen PSFF.

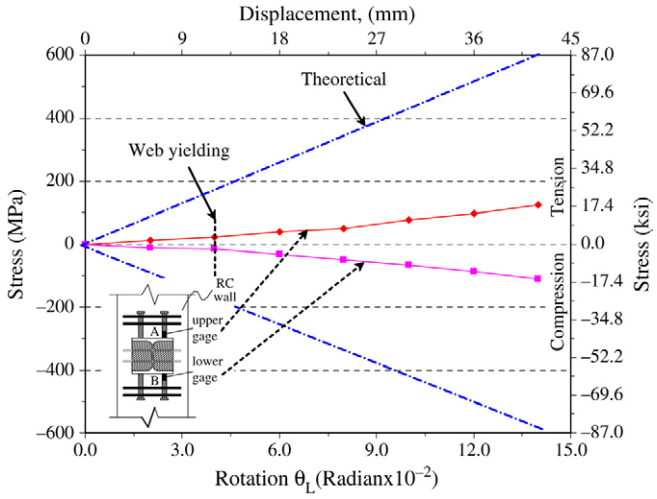

(c) Specimen PSFFT.

Fig. 11. Stresses of stud bolts.

Table 2
Test results

Specimen name	Detail of connection ①	②	③	Observed failure mode	Panel shear strength (kN) Observed average values $V_{(test)}$	Predicted values (ASCE Guideline) [7] $V_{n(ASCE)}$	Comparison ratio[a]	$V_{(test)}/V_{n(ASCE)}$
PSF	•	–	–	Panel shear failure	192.2	189.4	1.00	1.14
PSFF	•	•		Panel shear failure	282.4	265.9	1.47	1.06
PSFFT	•	•	•	Panel shear failure	342.6	316.9	1.78	1.08

①ST: Stud bolts; ②FBP: Face bearing plate; ③HT: Horizontal ties.
[a] Normalized value by standard specimen PSF.

horizontal force from the beam flanges into the concrete. A detailed analysis of specimen PSF indicated that roughly 80% of its shear strength was contributed by the steel web, and 20% by the concrete.

Specimens PSF and PSFF demonstrate the effectiveness of the face bearing plates in mobilizing the concrete compression strut. In specimens PSFF, face bearing plates as wide as the beam flange mobilized the concrete compression strut in the inner connection region. The panel shear strength of specimen PSFF could develop a shear force of 291 kN in the compression cycles (beam push down). Panel shear strengths of 50% above that of specimen PSF were measured. The face

bearing plate details increased the strength of the plain steel beam by 50% by developing the concrete compression strut mechanism. This significant increase in panel shear strength was attributed to the mobilization of concrete compressive struts inside the width of the steel coupling beam flanges. Based on the observation of the test results from a previous study [6], the thickness and configuration of the FBPs did not have significant effects on their performance. The results showed that the concrete compression strut width, and therefore its strength, was proportional to the width of the FBPs.

5.2. Concrete compression field

Specimens PSFF and PSFFT demonstrated the participation of the concrete compression field outside the beam flange. Recall that the concrete compression field is mobilized through horizontal transfer struts such as those shown in Fig. 4. Specimen PSFFT, which had FBPs and horizontal ties attached within the steel coupling beam depth, carried a load 19% greater than that of specimen PSFF. This is attributed to the concrete confinement effect of two-part U-shaped horizontal ties passing through holes drilled in the web of the steel coupling beam. Comparison of the capacity of specimens PSF and PSFF with that of specimen PSFFT indicated that about 50% of the increase could be attributed to the FBPs between the flanges, and the remainder, 19%, could be attributed to the horizontal ties within the steel coupling beam depth.

The contribution of each mechanism to the connection strength in specimen PSFFT is shown in Fig. 12. As shown in Fig. 12, the steel web and inner concrete panels were the two mechanisms that contributed the most to the shear strength of the steel coupling beam–wall connections. The contribution of the steel web panel to shear strength exceeded 40% beyond embedded web yielding. At a rotation angle of 0.002 rad, the deformation to connection strength at which yielding had occurred over most of the steel web panel exceeded 50% of the total shear. For larger shear distortions, this contribution diminished slightly because of the increase in the contribution of the inner concrete strut, reaching a minimum of 50% at 11% connection shear deformation. The contribution from the inner diagonal concrete strut also represented approximately 37% of the total connection at 11% joint shear deformation, and the contribution from the outer concrete strut represented approximately 13% of the joint shear capacity for all levels of joint shear deformation.

6. Comparison of test results and ASCE design guidelines

Fig. 13 and Table 3 show the $V_{(\text{test})}/V_{n(\text{ASCE})}$ ratio for all the test specimens, but applying the shear panel strength equations given in the ASCE guidelines [7]. For most of the specimens shown in this figure, the $V_{(\text{test})}/V_{n(\text{ASCE})}$ ratio ranged between 0.92 and 1.54. For specimen PSF, a 14% underestimation of the shear strength was obtained using ASCE guidelines. On the other hand, these guidelines predicted only 6% underestimation of the shear panel strength of specimen PSFF. This underestimation of the connection strength was

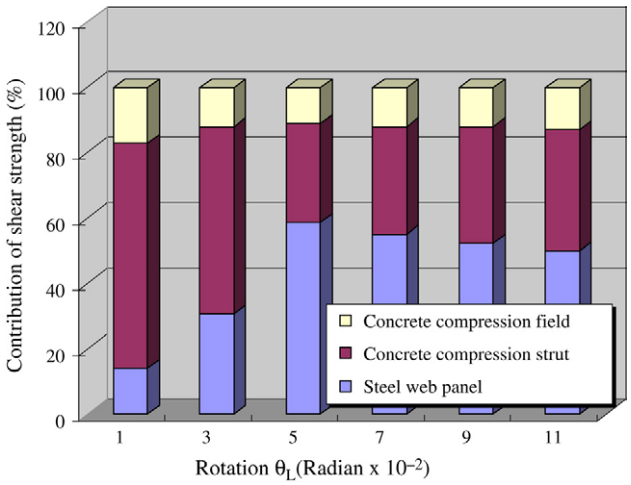

Fig. 12. Percentage contribution of shear strength mechanisms (specimen PSFFT).

because of the fact that no stirrups were used in the connection region. Therefore, only the concrete contribution from the concrete compression field described in the ASCE guidelines was obtained for the outer concrete panel. The lowest ratio was 0.92, obtained for specimen 1 by Montesinos et al. [16]. The highest ratio was 1.54, obtained for Kanno's specimen OJS2-0 [15]. For specimen OJS2-0, no shear keys were used to transfer shear forces to the outer connection regions. Thus, the only contribution to shear strength from the concrete in the ASCE guidelines would be given by the inner concrete panel between the steel beam flanges. However, it is very likely that a slightly wider region would have been mobilized by the face bearing plates, thus leading to the underestimation of the shear panel strength of the connection. A similar situation also occurred for specimens 10 and 11 by Deierlein and Noguchi [13], but underestimation of the shear panel strength was less significant.

As shown in Fig. 13, the average values of the ratio of $V_{(\text{test})}/V_{n(\text{ASCE})}$ for specimens PSF, PSFF, and PSFFT of 1.14, 1.06, and 1.08 were obtained, respectively. The predicted values from the ASCE design guidelines are generally in good agreement with the measured strengths. Therefore, based on the test results, the ASCE design guidelines may be applied as equations for predicting the panel shear strength of steel coupling beam–wall connections.

7. Conclusions

The following conclusions were derived from the results of studies on the panel shear strength of steel coupling beam–wall connections in a hybrid coupled shear wall system:

(1) All specimens exhibited severe damage in the connection region at the end of testing. From the observed failure modes, specimen PSFFT, with face bearing plates and horizontal ties in the panel region, was a more viable candidate than specimens PSF and PSFF for rehabilitation or retrofitting when considering the degree of building damage.

(2) Comparison of the capacity of specimens PSF and PSFF with that of specimen PSFFT indicated that about 50% of the

Table 3
Comparisons of other test results

Researcher	Specimen name	Observed value (kN)	Predicted value (kN)	Observed/Predicted	Failure mode
Sheikh et al. (1989)	Specimen 4	118.4	107.6	1.10	PF[a]
	Specimen 5	125.5	107.3	1.17	PF
	Specimen 7	150.4	139.3	1.08	PF
	Specimen 8	205.6	197.7	1.04	PF
	Specimen 10	129.1	112.2	1.15	PF
	Specimen 11	209.2	199.2	1.05	PF
Montesinos et al. (2003)	Specimen 1	166.0	180.4	0.92	PF
	Specimen 2	148.0	107.6	1.05	PF
	Specimen 4	192.0	107.6	1.06	PF
Kanno and Deierlein (2002)	OJS2-0	1731.0	1125.2	1.54	PF
	OJS3-0	2082.0	1582.3	1.32	PF
	OJS5-0	2299.0	1862.2	1.23	PF
	OJS7-0	2408.0	1613.4	1.49	PF
	HJS1-0	2534.0	2204.6	1.15	PF
	HJS2-0	2535.0	1977.3	1.28	PF
Noguchi and Kim (1998)	IN-1	715.0	707.9	1.01	PF
	EX-3	564.0	575.5	0.98	PF
Park and Yun (2005)	PSF	192.2	189.4	1.14	PF
	PSFF	282.4	265.9	1.06	PF
	PSFFT	342.6	316.9	1.18	PF

[a] PF: Panel shear failure.

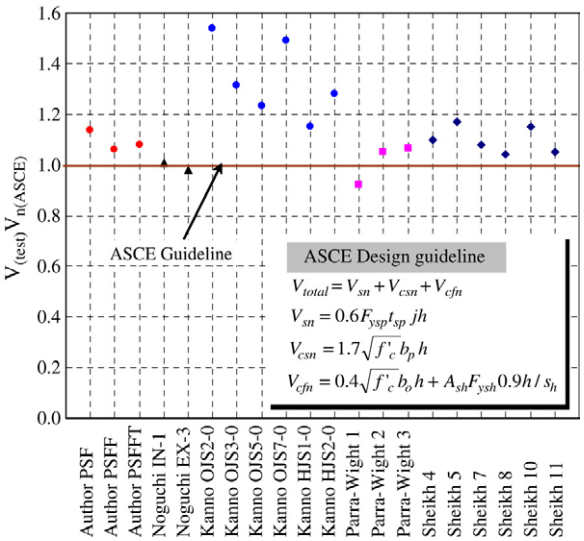

Fig. 13. Comparison of observed strength and predicted values by ASCE guidelines.

increase could be attributed to the FBPs between the flanges, and the remainder, 19%, could be attributed to the horizontal ties within the steel coupling beam depth.

(3) The distribution of steel web stresses does not follow a symmetrical pattern, with the higher stresses recorded in the front half of the embedded steel coupling beam length. Compared with specimens PSF and PSFF, the distributions of steel web stresses in specimen PSFFT were sensitive to the changes in the connection detail.

(4) Based on the observation of the horizontal strain for specimen PSFFT, the pre-cracking behaviour is characterized by negligible strains because of the small tensile stresses acting in the connection. After the first crack occurred, the tensile stresses previously acting in the concrete were primarily resisted by the horizontal ties.

(5) The average values of the ratio of $V_{(\text{test})}/V_{n(\text{ASCE})}$ obtained for specimens PSF, PSFF, and PSFFT were 1.14, 1.06, and 1.08, respectively. The predicted values from the ASCE guidelines are generally in good agreement with the measured strengths. Therefore, based on the test results, the ASCE design guidelines may be applied as equations for predicting the panel shear strength of steel coupling beam–wall connections.

Acknowledgement

This work was supported by the Korea Research Foundation Grant funded by the Korean Government (KRF-2005-214-D00381).

References

[1] Park WS, Yun HD. Seismic performance of steel coupling beam–wall connections in panel shear failure. Journal of Constructional Steel Research 2005, doi:10.1016/j.jcsr.2006.01.005.
[2] Park WS, Yun HD, Hwang SK, Han BC, Yang IL. Shear strength of connection between steel coupling and reinforced concrete shear wall in a hybrid wall system. Journal of Constructional Steel Research 2005;61(7): 912–41.
[3] Park WS, Yun HD. Seismic behaviour of steel coupling beam linking reinforced concrete shear wall. Engineering Structure 2005;27(7): 1024–39.
[4] Park WS, Yun HD. Seismic behaviour of coupling beam in a hybrid coupled shear walls. Journal of Constructional Steel Research 2005; 61(11):1492–524.
[5] Deierlein GG, Yura JA, Jirsa JO. Design of moment connections for composite framed structures. PMFSEL; Report no. 88-1, Austin, Tex: The University of Texas as Austin; 1988.
[6] Sheikh TM, Deierlein GG, Yura JA, Jirsa JO. Beam-column moment connections for Composite Frames: Part 1. Journal of Structural Engineering, ASCE 1989;115(11):2858–76.

[7] ASCE Task Committee on Design Criteria for Composite Structures in Steel and Concrete. Guideline for design of joints between steel beams and reinforced concrete columns. Journal of Structural Engineering, ASCE 1994;120(8):2330–51.
[8] Nishiyama I, Kuramoto H. Inelastic force-deformation response of joint shear panel in beam-column moment connections to concrete-filled tubes. Journal of Structural Engineering, ASCE 2004;130(2):244–52.
[9] Kuramoto H, Nishiyama I. Seismic performance and stress transferring mechanism of through-column-type joints for composite reinforced concrete and steel frame. Journal of Structural Engineering, ASCE 2004; 130(2):352–60.
[10] Yoshino T, Kanoh Y, Mikame A, Saski H. Mixed structural systems of precast concrete columns and steel beams. In: IABSE Symp. Proc.: mixed structures including new materials, International Association for Bridge and Structural Engineering; 1990: p. 401–6.
[11] Noguchi H, Uchida K. Finite element method analysis of Hybrid structural frames with reinforced concrete columns and steel beams. Journal of Structural Engineering, ASCE 2004;130(2):328–35.
[12] Noguchi H, Kim K. Shear strength of beam-to-column connections in RCS system. In: Proceedings of structural engineers world congress. Elsevier Science, Ltd.; 1998. Paper No. T177-3.
[13] Deierlein GG, Noguchi H. Overview of US–Japan research on the seismic design of composite reinforced concrete and steel moment frame structures. Journal of Structural Engineering, ASCE 2004;130(2):361–7.
[14] Sheikh TM, Yura JA, Jirsa JO. Moment connections between steel beams and concrete columns. PMFSEL Report No. 87-4, Austin, Tex: The University of Texas at Austin, 1987.
[15] Kanno R, Deierlein GG. Design model of joints for RCS frames. Conference of Proceeding. Journal of Structural Engineering 2002; 947–58.
[16] Parra-Montesinos G, Liang X, Wight JK. Toward deformation-based capacity design of RCS beam-column connections. Journal of Engineering Structure 2003;25(5):681–90.
[17] Moore W, Goasain N. Mixed systems: Past practices, recent experience and future direction. In: Roeder C, editor. Composite and mixed construction. New York: ASCE; 1985. p. 138–49.